SECTION 9.16
SOLIDS PUMPING

9.16.1
HYDRAULIC TRANSPORT OF SOLIDS

KENNETH C. WILSON
ANDERS SELLGREN

INTRODUCTION

Applications of Slurry Transport Vast tonnages are pumped every year in the form of solid-liquid mixtures, known as slurries. The majority of applications are short-distance in-plant installations, mainly in the minerals industry. A large plant may contain several hundred centrifugal pumps handling various types of slurries.

The application that involves the largest quantities is the dredging industry, continually maintaining navigation in harbors and rivers, altering coastlines and winning material for landfill and construction purposes. As a single dredge may be required to maintain a throughput of 7000 tons of slurry per hour or more, very large centrifugal pumps are used with impeller diameters of over 100 in. (2.5 m). (See Wilson et al., 1997, and Subsection 9.16.2.)

The manufacture of fertilizer is another process involving massive slurry-transport operations. In Florida phosphate matrix is recovered by huge draglines in open-pit mining operations. It is then slurried, and pumped to the wash plants through pipelines with a typical length of about 6 miles (10 km). The total drive capacity can be in excess of 13,400 hp (10 MW).

Recent decades have seen a great increase in the transport of waste materials, in slurry form, to suitable deposit sites. Waste-disposal environmental problems require that wastes be conveyed to dedicated and monitored disposal sites, either underground or on the surface. This requirement can often be satisfied by backfilling mines (either deep or open-pit), and slurry transport is the favored placing method.

Large slurry pumping operations are found in Alberta, Canada, where oil sands obtained by open-pit mining operations are directly pumped for processing. The mixing and exposure time during the slurry transportation has eliminated some of the processing carried out at the processing plant, resulting in large savings. After the extraction operations are completed, the sand is used as backfill in areas previously mined.

Coarse-particle slurries with maximum particle sizes of 4 inches (100 mm) or more can often be pumped cost-effectively by combining them with smaller particles, to produce a broad and even particle size distribution (Sellgren & Addie, 1998).

Slurry transportation may play an important role in the development of integrated mining systems of tomorrow. In mines there is sometimes a considerable inflow of groundwater that has to be removed. When the mine dewatering installations are integrated with a hydraulic hoisting system, the cost of power needed to pump out the groundwater can be excluded from the cost of hoisting in making cost comparisons with other modes of transporting the solids to the surface. The economic effectiveness of hydraulic hoisting, together with hydraulic design considerations, have been discussed by Kostuik (1965) and Sellgren et al. (1989) for both small shallow mines and large deep underground mines.

Long-distance slurry pipeline transport is a thoroughly tested and cost-effective mode of transportation of ores, coal, and industrial minerals. For example, in Brazil up to 13 million tons (12 million tonnes) of iron ore concentrate (0.15 mm) have been pumped per year since 1977 from an inland mine to a pellet plant at the coast 250 miles (400 km) away. The well-known Black Mesa pipeline in southwestern United States transports a partially processed slurry coal (1.5 mm) about the same distance to an electrical generating station.

Long distance slurry pipelines involve heads of 75 atmospheres or more at each pumping section, the pumps employed are therefore usually of the positive-displacement type (see Subsection 9.16.3). Descriptions of long-distance pipelines and associated slurry pumps can be found, for example, in Brown & Heywood (1991).

Principles of Slurry Flow Slurries are mixtures of solid particles and a liquid (typically water). The interaction of the solids and the liquid can produce a large variety of flow behaviors. The major types will be outlined here and described in more detail in subsequent sections. The simplest type of slurry behavior occurs, for example, when silt or fine sand is dredged. It is represented by the "equivalent fluid" model. This evaluates the friction loss (pressure gradient) in the pipeline on the basis of an equivalent fluid with the density of the mixture and a friction factor near that of water at the same flow rate. This simple case is not particularly common in practice. On one hand, there are slurries of finer particles, e.g., natural clays or industrial materials like red mud. Typically, these are non-Newtonian in nature, and require rheological techniques to evaluate the pressure gradient. These will be outlined in the following section on homogeneous slurries.

On the other hand, as particle size or density increases, then settling of particles becomes significant. In turbulent flow the fluctuating velocity of the turbulent eddies (v') acts against the particle settling velocity (terminal fall velocity v_t). The importance of particle settling increases as the ratio v_t/v' becomes larger. When settling is significant the slurry is no longer homogeneous. It is particle-lean near the top of the pipe and particle-rich near the bottom. In the lower area, contact between particles and the bottom of the pipe add a granular (Coulombic) shear stress to that produced by the fluid, thus increasing the pressure gradient (for a given flow rate). The solids contributing to this Coulombic stress are known as "contact load" solids. The stratification ratio, representing the fraction of total solids that travels as contact load, tends to increase with v_t/v'. The turbulent fluctuating velocity v' varies with the mean flow velocity V_m (flow rate divided by $\pi D^2/4$ where D is the internal pipe diameter). Thus, decreasing V_m from an initially large value increases the stratification ratio, and hence the solids effect on the pressure gradient. With further reductions in V_m the liquid effect on pressure gradient decreases, combining with the increasing solids effect to produce a minimum in the pressure gradient (for constant delivered solids concentration). This minimum, shown schematically on Figure 1, was observed long ago by Blatch (1906).

Calculations for this type of pressure-gradient behavior are outlined in the next section on settling slurries, as are other features of this type of flow. It is worth noting here that, as V_m is decreased below the minimum-gradient value, there comes a lesser velocity at which particles at the bottom of the pipe cease moving and form a stationary deposit, also shown on Figure 1. This deposit leads to a further increase in pressure gradient (and hence in the power required) and may cause system instability. Beginning with Durand (1951a, 1951b), deposition has been studied extensively (see the settling slurry section), primarily so that it can be predicted and hence avoided in engineering design.

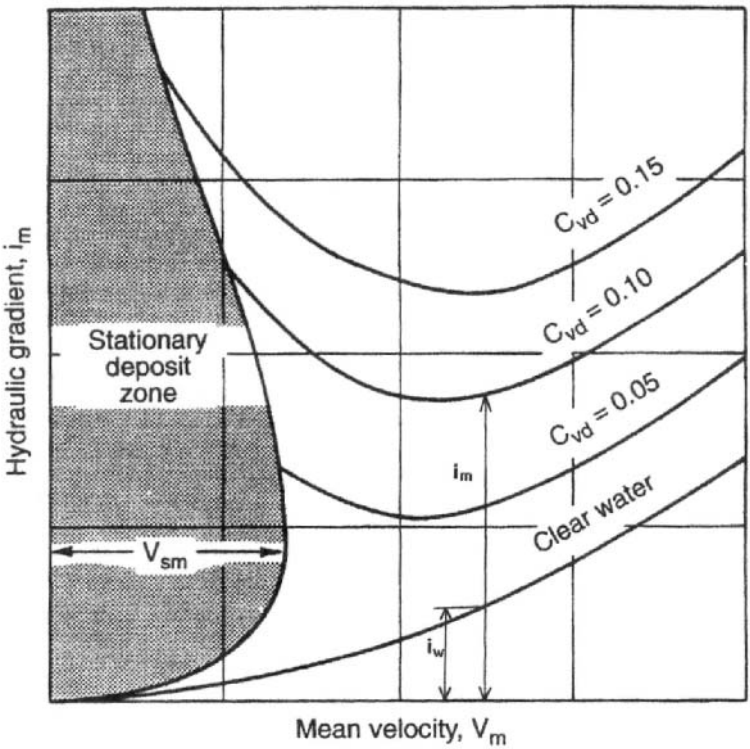

FIGURE 1 Definition sketch

Newitt et al. (1955) divided slurry flows into three types. These include the equivalent-fluid type and the partially stratified type, which have been previously described. The remaining type is known as fully stratified. In this case, either the particle fall velocity is large or the particle size is a significant fraction of the pipe diameter. These factors preclude any support of the solids by the fluid turbulence, so that the submerged weight of all the particles must be carried to the pipe by granular contacts. Calculations (outlined on the section on settling slurries) and experiments show that pressure gradients can be very high for this type of flow. As a result, it is not suitable for long-distance or medium-distance transport; but it has found some applications for short hauls.

HOMOGENEOUS SLURRIES

Equivalent-Fluid Calculations As mentioned in the previous section, pseudo-homogeneous flow (for example aqueous slurries of silt or fine sand) shares with truly homogeneous flow the property that the pressure gradient increases with througput velocity in a fluid-like fashion. An increase of this type can be expressed, at least to a reasonable approximation, by the statement that the pressure drop for turbulent flow of a homogeneous or pseudo-homogeneous mixture is proportional to that obtained for an equal discharge of carrier fluid alone.

Before this statement can be put into mathematical form, it is necessary to consider various ways of expressing the pressure drop due to friction. The change of pressure per

unit length of pipe, $\Delta p/\Delta x$, is not commonly employed in practice, in part because it includes the effect of differences in elevation as well as friction losses. For liquids, especially water, the hydraulic gradient, i, is normally used. This quantity is the slope of the hydraulic grade line, which is based on the levels to which the fluid would rise in a series of imaginary tubes tapped into the pipeline. As the slope of the hydraulic grade line, the hydraulic gradient represents the drop in level per unit length of pipe. For water (density ρ_w) flowing in a horizontal pipe, i is related to the pressure gradient as follows

$$i = \left(- \frac{\Delta p}{\Delta x} \right) / \rho_w g \tag{1}$$

where g is gravitational acceleration.

As water forms the carrier liquid in the majority of slurry flows, it is convenient to use it as a standard for comparison of frictional pressure losses. Thus, throughout this chapter the usual expression for frictional losses is in terms of i (height of water per unit length of pipe). The value for i for clear-water flow is written i_w, and that for a mixture (i.e. frictional loss in height of water per unit length) is written i_m. The statement made previously for homogeneous and pseudo-homogeneous flows amounts to a direct proportionality between i_m and i_w.

Calculation of i_w uses the Stanton-Moody friction factor, f, in the equation

$$i_w = f \frac{V^2}{2gD} \tag{2}$$

For turbulent flow, the friction factor depends on both the Reynolds number ($Re = \rho V_m D/\mu$) and the relative roughness ε/D. These two quantities can be entered on Figure 2, which is

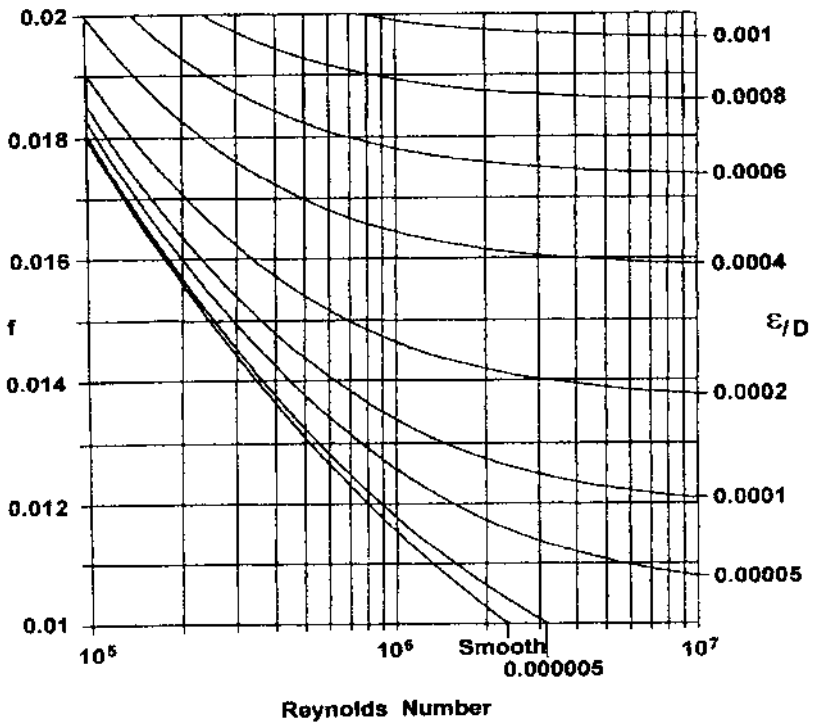

FIGURE 2 Friction factor in normal operating range

used to obtain f. For example, with $Re = 1.5 \times 10^6$ and $\varepsilon/D = 0.0001$, $f = 0.013$ (a typical value). As f is approximately constant for turbulent flow in a given pipe, Eq. 2 shows that the hydraulic gradient varies roughly as V^2 (or as Q^2).

In non-slurry applications, if a liquid other than water is conveyed, the hydraulic gradient concept is applied by substituting the density of this liquid for that of water in Eq. 1, so that the hydraulic gradient is expressed in height of flowing liquid per unit length. In considering, say, a pseudo-homogeneous slurry of fine sand, it may be of interest to compare its behavior to that of a liquid with density equal to that of the flowing mixture ρ_m, which is given by

$$\rho_m = \rho_w(1 + (S_s - 1)C_v) \tag{3}$$

Here S_s is the relative density of the solids (compared to water) and C_v is the volumetric concentration of solids.

Substituting ρ_m for ρ_w in Eq. 1 gives the mixture-height gradient (i.e. measured in height of mixture rather than of water). For clarity, a different symbol must be used, and j is employed for this purpose. For a mixture flowing in a horizontal pipe:

$$j = \left(- \frac{\Delta p}{\Delta x} \right) / \rho_m g \tag{4}$$

Although j is expressed in height of mixture per unit length of pipe, actual measurements based on columns of mixture in vertical tubes would not be feasible, and j would have to be obtained indirectly from pressure measurements. It can be seen from Eqs. 1 and 4 that the ratio of i to j equals the relative density of the mixture S_m (i.e. ρ_m/ρ_w).

The equivalent-fluid model of slurry flow assumes that the solids have little effect on friction factor, and that the mixture acts as a liquid as far as the relative-density effect is concerned. The resulting hydraulic gradient for homogeneous mixture flow, i_{mh}, is equivalent to the product of S_m and i_w. Although the equivalent-fluid model has been widely employed in the past, it is not generally supported by the experimental evidence. For example, sand-water experiments by Carstens & Addie (1981) show that for some pseudo-homogeneous flows i_{mh} does not exceed i_w at all. An appropriate equation for the hydraulic gradient is:

$$i_{mh} = [1 + A'(S_m - 1)]i_w \tag{5}$$

Setting the coefficient A' equal to unity gives the relative-density effect of an equivalent-fluid model, whereas $A' = 0$ gives the behavior observed by Carstens & Addie (1981). Intermediate types can be represented by values of A' between zero and unity. Equation 5 will be referred to as the "homogeneous flow" equation, with the specific case of $A' = 1.0$ called the "equivalent fluid" model.

Modeling Non-Newtonian Flows In pipeline transport of non-Newtonian materials, the variation of pressure drop with velocity is typically rather flat for laminar flow, while it is much steeper for turbulent flow. Figure 3 shows these features. This figure is a plot, on logarithmic axes, of hydraulic gradient j_m (i.e. frictional losses in height of equivalent fluid per unit length of pipe) versus mean velocity V_m (volumetric discharge/cross-sectional area). The data shown on this plot refer to various concentrations of a red mud tested at the GIW Hydraulic Laboratory in a pipeline with internal diameter of 3.19 in. (81 mm). The plotted data are for mixtures with relative densities from 1.14 to 1.28. Note that where laminar flow occurs the slope of the lines (referred to the logarithmic coordinates) is rather small and does not vary significantly with particle concentration. However, the vertical position of the laminar lines increases strongly with increasing concentration. Conversely, for turbulent flow, concentration has very little effect; all the points fall close to a single line with slope (for logarithmic coordinates) close to 2.0. This behavior implies that the friction factor f has a near-constant value for the observed turbulent flows. Note that the transitions between laminar and turbulent flow are rather abrupt.

Rheograms, i.e. curves of shear stress versus strain rate, are obtained from tests under laminar conditions, using either rotary viscometers or tube viscometers. The latter are

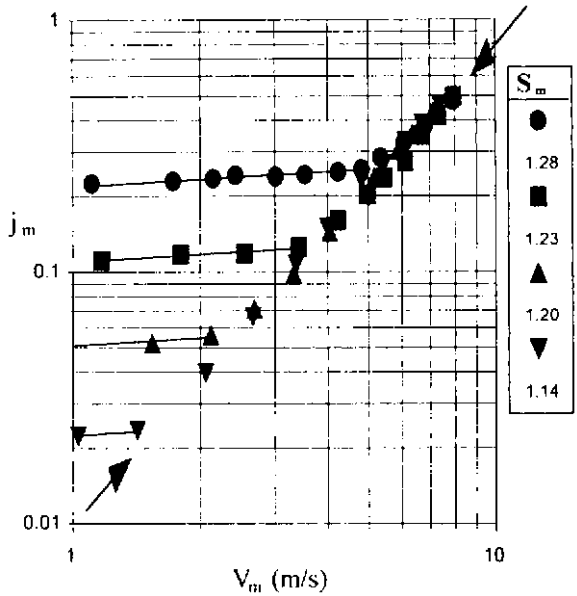

FIGURE 3 Friction gradients of a red-mud slurry

preferable, as they are geometrically similar to the pipeline configuration. For a Newtonian fluid of viscosity μ, shear stress τ is related to strain rate du/dy by the classic expression

$$\tau = \mu(du/dy) \tag{6}$$

Rheograms for non-Newtonian materials are not so simple. For example, Figure 4 shows a rheogram for a fine-particle slurry. This rheogram does not pass through the origin (the strain rate remains zero until a certain yield stress τ_y is exceeded) and is not straight (although in this case the behavior is approximately linear at large values of strain rate). The definition of viscosity given by Eq. 6 can be retained, although this viscosity no longer represents the slope of the rheogram itself, but rather that of the secant line shown on the figure. Hence μ as defined by Eq. 6 can also be called the "secant" viscosity. The tangent to the rheogram, though less meaningful physically, is often referred to. This "tangent" viscosity will be denoted η_t. Both μ and η_t vary with position, and hence they both depend on du/dy (or, alternatively, on τ). The stippling of Figure 4 indicates the area beneath the leftward portion of the rheogram. The area ratio α (which will be used below) is the ratio between the stippled area and the traingular area below the secant line. As with μ and η_t, both the area beneath the rheogram and the area ratio α depend on du/dy (or on τ).

It is common practice to represent rheograms by simple mathematical functions (i.e. functions having only two or three parameters). For materials exhibiting a yield stress, the most common engineering choice is the Bingham model, a straight line given by

$$\tau = \tau_B + \eta_B(du/dy) \tag{7}$$

Here the Bingham viscosity η_B is the tangent viscosity given by the slope of the fit line, and the Bingham yield stress τ_B is the intercept of the fit line with the shear-stress axis. For the data of Figure 4, τ_B is larger than the observed stress at zero strain rate, a situation that is commonly encountered.

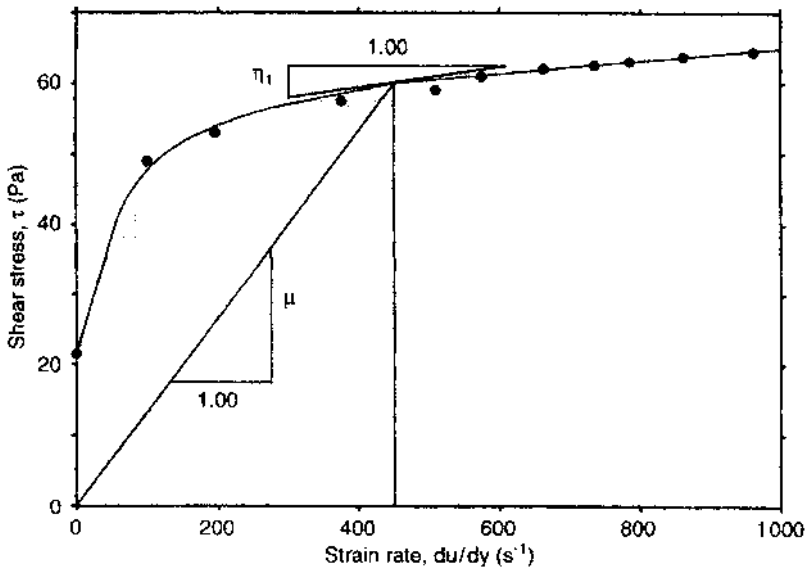

FIGURE 4 Rheogram for phosphate slimes tested at GIW Hydraulic Laboratory (after Wilson, 1986). [Pa × 0.000145 = lb/in^2]

The dimensionless ratio τ/τ_B (denoted θ and called the stress ratio) is a useful parameter when dealing with Bingham physics. For example, in laminar flow, the secant viscosity ("apparent viscosity") μ is related to the stress ratio by the equation

$$\mu/\eta_B = \theta/(\theta - 1) \tag{8}$$

This equation indicates a gradual decrease of μ with increasing stress ratio. Another parameter appropriate for Bingham plastics is the Hedström number, *He*

$$He = D^2\rho\tau_B/\eta_B^2 \tag{9}$$

where ρ is the mixture density.

The friction factor for laminar flow of a Bingham plastic can be expressed in terms of these parameters as

$$\sqrt{\frac{8}{f}} = \sqrt{He}\cdot\left(1 - \frac{4\theta^{-1}}{3} + \frac{\theta^{-4}}{3}\right)\cdot\frac{\sqrt{\theta}}{8} \tag{10}$$

As noted previously, turbulent flows of non-Newtonians are often characterized by a roughly constant value of friction factor, in contrast with the large variations typical of laminar flow. An old way of estimating *f* for turbulent flow, proposed by Hedström (1952), is to use the Bingham viscosity η_B in place of μ in the relationship for Newtonian turbulent flow. This approach should be considered as only a rough approximation. A better method is to begin with, say, the smooth-wall Newtonian equation

$$V_m = 2.5U_*\ell n(\rho DU_*/\mu) \tag{11}$$

where ℓn denotes the natural logarithm and the shear velocity U_*, i.e. $\sqrt{\tau/\rho}$, is evaluated at the pipe wall. For turbulent pipe-flow tests of a non-Newtonian material, all quantities except μ will be available for each test run. Therefore, in each case Eq. 11 can be solved for

the viscosity, which is now denoted μ_{eq}, the equivalent turbulent-flow viscosity. This viscosity is not constant (as would be the case for a Newtonian fluid, or for Hedström's postulate, i.e. $\mu_{eq} = \eta_B$) but varies with wall shear stress, and hence with shear velocity, as described by Wilson et al. (1997).

If turbulent-flow tests are available, scale-up to prototype size can be accomplished directly (as shown in the following section). Otherwise, μ_{eq} can be predicted on the basis of the laminar-flow rheogram. The prediction method follows the model of Wilson & Thomas (1985), which in turn is based on a proposal of Lumley (1973, 1978) regarding the viscous sub-layer. Increasing the size of the dissipative micro-eddies leads to an increase in the thickness of this sub-layer. The thickened sub-layer, in turn, produces a higher mean velocity for the same wall shear stress. The model uses the ratio of the integrals under the non-Newtonian and Newtonian rheograms (denoted by α, and defined earlier in connection with Figure 4) to estimate the size increase of the turbulent micro-eddies. It is found that both the micro-eddy size and the thickness of the viscous sub-layer should be multiplied by a factor equal to α. This results in a simple expression for the equivalent turbulent-flow viscosity. For a Bingham plastic α can be expressed in terms of the stress ratio as $(\theta + 1)/\theta$, and the expression for μ_{eq} becomes

$$\mu_{eq}/\eta_B = [(\theta + 1)/(\theta - 1)]\exp(-4.64/\theta) \tag{12}$$

A plot of this function (Wilson, 1997) shows that, as θ increases above 1.0, μ_{eq}/η_B begins by dropping below unity, descends to a minimum (0.216 at $\theta = 1.32$) and then rises gradually toward unity. The resulting expression for turbulent-flow friction factor depends only on the parameters *He* and θ. The equivalent expression for laminar flow (Eq. 10) involves the same two parameters. The intercept of turbulent and laminar lines occurs where these two equations give the same value of *f*. At this intercept it is possible to eliminate θ using an iterative technique, thus producing a plot of *f* (at intercept) versus Hedström number. On logarithmic coordinates the plot is not far from a straight line in the region $200 \leq \sqrt{He} \leq 10000$, and a power-law approximation can be used in this range, as follows:

$$f \approx 0.0877(He)^{-0.113} \tag{13}$$

Experimental evidence from pipe-flow tests of fine-particle slurries typically shows abrupt laminar-turbulent transitions, followed in the turbulent range by a plateau of virtually constant friction factor. Equation 13 gives a valuable tool for predicing *f* for this plateau. This friction factor falls below the traditional curve of Hedström, by which the equivalent turbulent-flow viscosity is equated to the Bingham tangent viscosity, η_B.

This technique can be extended to predict the transition between laminar and turbulent flow. For a Newtonian fluid, with a single rheological parameter (μ), the transition is defined by a specific value of a single dimensionless ratio (the Reynolds number $\rho V_m D/\mu$). A second rheological parameter, required for a non-Newtonian material such as a Bingham plastic, introduces the need for a second dimensionless ratio. In this case the two ratios are the "Bingham" Reynolds number, i.e. $Re_B = \rho V_m D/\eta_B$ and Hedström number which has been previously defined. As pointed out by D. G. Thomas (1963) the laminar-turbulent transition must now be defined by a functional relationship linking Re_B at transition with *He*.

Following the method used in obtaining Eq. 13, the laminar and turbulent relations can be equated at the intercept and *f* (as well as θ) can be eliminated to obtain a plot of Re_B at intercept versus *He*. It was found that the result could be closely approximated by the simple relationship that Re_B equals $25\sqrt{He}$. On cancelling common quantities, it is seen that the flow velocity at transition, say V_T, is given by:

$$V_T \cong 25\sqrt{\tau_B/\rho} \tag{14}$$

The approach of D. G. Thomas (1963) produced a similar form in the limit, but with a coefficient of 19 rather than 25.

Scale-up of Laminar and Turbulent Flows The laminar flow of any given fluid can be scaled from one pipe size to another by use of the Rabinowitsch-Mooney technique provided that the flow remains laminar in both pipes (turbulent flow will be dealt with separately below). The basis of the Rabinowitsch-Mooney technique is the plot of wall shear stress τ_0 versus $8V_m/D$. Rabinowitsch (1929) and Mooney (1931) proved that for steady uniform laminar flows in a pipe τ_0 and $8V_m/D$ are linked in a functional relationship. In other words, for a given material the values of both τ_0 and $8V_m/D$ can be determined from experiments in a single pipe. The experimentally determined plot or function linking these two variables can then be applied to all laminar flows of the material in question, whatever the pipe diameter.

The application of the method is based on a logarithmic plot of τ_0 versus $8V_m/D$ obtained from a pipe of internal diameter D_1. For some other pipe, of diameter D_2, the pressure gradient dp/dx can be obtained from the plotted values of τ_0 by multiplying them by $(4/D_2)$. Since the factors by which each of the coordinates are multiplied depend only on D_2, a simple re-scaling of the axes of the figure based on D_1 gives a plot of dp/dx versus V_m for a pipe of diameter D_2. For plots on logarithmic coordinates, this type of scaling amounts to a pair of linear translations, which do not affect the shape of the plot. In this regard it should be noted that a Newtonian fluid shows a slope of unity on a logarithmic plot of pressure gradient versus mean velocity, whereas the slopes of logarithmic plots for non-Newtonian laminar flow (such as those on Figure 3) are much flatter.

An alternative way of dealing with scale-up to a larger pipe is to transform the data from the experimental pipe (diameter D_1) to the prototype (diameter D_2) on a point-by-point basis. This process is similar to using the affinity laws for scaling head and discharge data for a centrifugal pump. For the pipe, the analogous quantities are the frictional gradient i_m (ft of water/ft or m of water/m) and the mean velocity V_m. With the subscripts 1 and 2 denoting experimental and prototype conditions, respectively, the scaling relations (affinity laws) for laminar flows in pipes are:

$$(i_m)_2 = (i_m)_1 \left(\frac{D_1}{D_2}\right) \tag{15}$$

and

$$(V_m)_2 = (V_m)_1 \left(\frac{D_2}{D_1}\right) \tag{16}$$

If it is foreseen that flow in the prototype pipeline may be turbulent, it is important to extend the small-scale experimental tests into the turbulent-flow region, and then to scale these test results up to prototype size. For turbulent scaling, as for the laminar case, the quantity that remains unchanged is the wall shear stress τ_0. As in laminar flow, the wall shear stress fully determines the stress distribution within the pipe. For example, with a material having a yield stress τ_y a specified value of τ_0 is sufficient to give the fraction of the pipe area where $\tau < \tau_y$, a factor which can affect the mean velocity (Wilson & Thomas, 1985; Thomas & Wilson, 1987). Likewise, a given value of τ_0, and hence of U_*, determines conditions within the viscous sub-layer and hence establishes both μ and the area ratio α. The result is that τ_0 (or U_*) is sufficient to determine the equivalent turbulent-flow viscosity. For each value of τ_0 two scaling laws apply to turbulent pipe flow. The first, for pressure gradient, is the same as that established for laminar flow, i.e. Eq. 15. The second scaling law, for mean velocity, is given by

$$(V_m)_2 = (V_m)_1 + 2.5U_* \ell n(D_2/D_1) \tag{17}$$

As with Eqs. 15 and 16 for laminar flow, the combined use of Eqs. 15 and 17 allow scale-up of data for turbulent non-Newtonian flow from one pipe size to another. Wilson (1986) gives an example where scaled-up values from a small pipe are compared to measured data in a larger pipe, with very satisfactory agreement. Equation 17 is also valid for cases where μ is constant, i.e. for Newtonian fluids, and for turbulent flow of dilute polymer solutions exhibiting drag reduction (Wilson, 1989).

TABLE 1 Data for phosphate slimes slurry in 8 in. (203 mm) pipe

	V_m				τ_0		U_*	
Run	ft/s	m/s	$8V_m/D(s^{-1})$	i_m	lb/ft^2	Pa	ft/s	m/s
1	1.7	0.53	21.0	0.1004	1.04	49.9	0.69	0.210
2	5.0	1.52	60.1	0.1130	1.17	56.2	0.73	0.223
3	6.6	2.00	78.8	0.1150	1.19	57.2	0.74	0.225
4	8.5	2.59	102.1	0.1189	1.24	59.1	0.75	0.229
5	10.6	3.24	127.9	0.1218	1.27	60.1	0.76	0.231
6	12.5	3.81	150.3	0.1237	1.29	61.5	0.77	0.233
7	14.5	4.43	174.7	0.1273	1.32	63.4	0.78	0.237
8	16.8	5.12	202.0	0.1348	1.40	67.0	0.80	0.243
9	18.5	5.64	222.6	0.1472	1.53	73.2	0.83	0.254

EXAMPLE 1 A clay-water slurry of phosphate slimes is to be pumped over a horizontal distance of 2300 ft. (700 m), using a pipe of internal diameter 12 in. (305 mm). The slurry will be taken from a pond in which the relative density of the mixture is 1 · 13. Tests have been carried out with this material using a pipe of internal diameter 8 in. (203 mm). Test data for i_m and V_m appear in Table 1 together with values of $8V_m/D$ and τ_0 (the wall shear stress equals $\rho_w g i_m D/4$). Figure 5 shows the values of i_m plotted versus V_m for the test pipe.

The preliminary design of the pumping system calls for a discharge Q_m of 4770 gpm (0.30 m^3/s) in the prototype pipe. However, this value is not yet definite, and Q_m values of 3180 gpm (0.20 m^3/s) and 6360 gpm (0.40 m^3/s) are also to be considered.

a. Find the values of i_m for the three values of Q_m just noted. First, the pipe area (0.785 ft^2 or 0.0731 m^2) is used to obtain the required velocities, i.e. 9.0, 13.5 and 18.0 ft/s (2.74, 4.11 and 5.48 m/s).

The next step is to scale the data points from the test pipe to the prototype pipe. For the laminar-flow points the appropriate scaling laws are given by Eqs. 15 and 16, which show that i_m scales inversely with the diameter ratio while V_m scales directly with this ratio. Points from test runs 1 to 7 have been scaled on this basis and the first six are shown on Figure 5. For test runs 8 and 9 the flow is turbulent. The hydraulic gradient can still be scaled by Eq. 15, but V_m must now be scaled by Eq. 17. This requires evaluation of U_*, i.e. $\sqrt{\tau_0/\rho}$. For example, run 8 with $\tau_0 = 0.01$ lb/ft^2 (67.0 Pa) has $U_* = 0.8$ ft/s (0.243 m/s), for which Eq. 17 gives a scaled-up value of V_m equal to 17.6 ft/s (5.37 m/s).

The laminar-turbulent transition point is obtained by projecting the turbulent line back to intercept the laminar line. For the data in the test pipe this intercept occurred to the right of point 7, at a velocity of about 16 ft/s (say 5 m/s). For the prototype pipe the intercept lies between points 4 and 5, with a slightly lower velocity. Note that the scaled values for points 5 to 7 are not physically meaningful, because the equivalent flows in the prototype pipe are turbulent, not laminar.

Figure 5 shows that conditions will be laminar for the two lower flows to be investigated, and turbulent for the highest flow. The values of i_m can be taken directly from the figure, and are listed in Table 2.

The flat curve for laminar flow, plotted on Figure 5, shows a very small rise in i_m as Q_m goes from 7.1 to 10.6 ft^3/s (0.20 to 0.30 m^3/s). On the other hand, the equal increase of Q_m from 10.6 to 14.1 ft^3/s (0.30 to 0.40 m^3/s) requires a much larger increment in i_m, as a result of the shift from laminar to turbulent flow.

b. Suppose now that testing had stopped after run 6, so that no turbulent-data flow points were available.

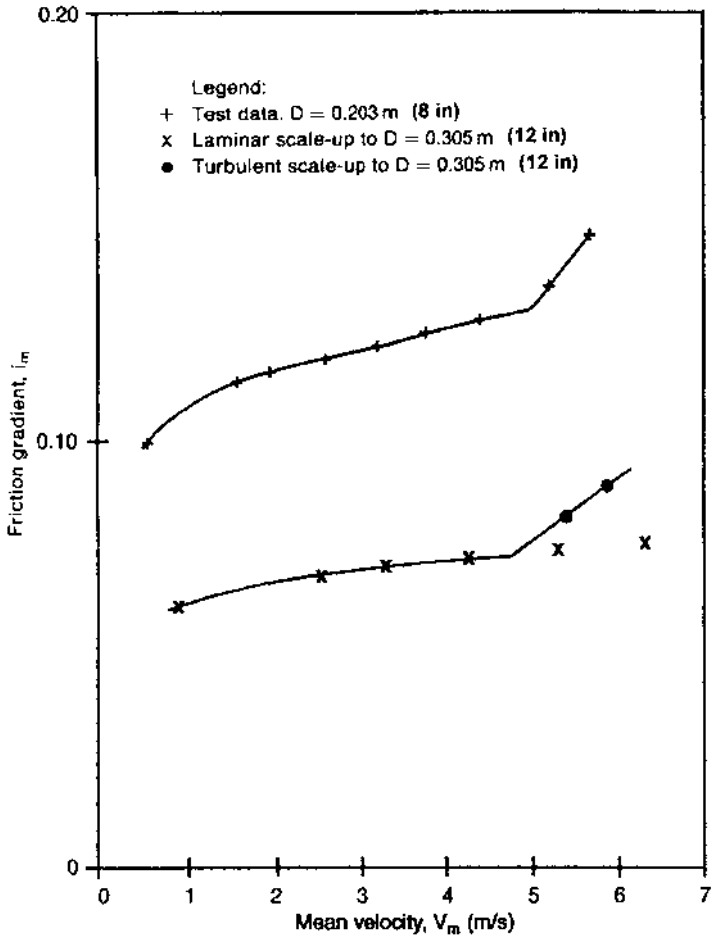

FIGURE 5 Test data and scale-up for Example 1. [m/s × 3.28 = ft/s]

TABLE 2 Hydraulic gradients and pump heads from scaled-up values

Q_m (m^3/s)	0.20	0.30	0.40
Q_m (US gpm)	3180	4760	6360
V_m (m/s)	2.74	4.11	5.48
V_m (ft/s)	9.0	13.5	18.0
i_m	0.0760	0.0795	0.0915
Pump Head (m water)	53.2	55.6	64.0
Pump Head (ft water)	174	183	210

In this case the laminar line would be scaled as before, but the transition to turbulent flow must be predicted from the parameters of the laminar-flow rheogram. It was found that all laminar points except the lowest one can be considered as

obeying a Bingham formulation of the rheogram, with $\tau_y = 0.0076$ lb/in^2 (52.7 Pa) and $\eta_B = 0.020$ Pa · s. Substitution of these quantities into Eq. 14 yields $V_T = 17.7$ ft/s (5.4 m/s) which is somewhat above the observed transition. The similar expression of D. G. Thomas (1963) gives V_T of 13.4 ft/s (4.1 m/s), significantly below the observed transition point. The use of Eq. 13 to evaluate turbulent friction produces a turbulent line that passes through the transition point predicted by Eq. 14.

SETTLING SLURRIES

Velocity at Limit of Stationary Deposition The deposition limit will be discussed in this section, and the modelling of fully-stratified coarse-particle flow at velocities above the deposition limit in the following section.

The results of a detailed force-balance computer model for the limit of stationary deposition showed that the throughput velocity V_m at this limit is concentration-dependent, having small values at low concentration, rising to a maximum (denoted V_{sm}) at some intermediate concentration (which depends on pipe size and particle size and density) and then dropping off again as the delivered solids concentration approaches the loose-poured value, C_{vb}. This behavior was shown on Figure 1. It should be noted that the velocities used here are obtained simply by dividing the mixture flow rate (Q_m) by the pipe area ($\pi D^2/4$).

The computer output is unwieldy for a designer concerned with many alternative proposals. Moreover, the conservative designer may be content to know only the maximum velocity at the limit of deposition, V_{sm}, since maintaining the operating velocity above this value ensures that deposition will not occur. The value of V_{sm} depends on internal pipe diameter, particle diameter and relative density, and the effect of these variables is expressed concisely by a nomographic chart which was developed at Queen's University (Wilson & Judge, 1978; Wilson, 1979) with the help of the late Professor F. M. Wood's expertise in nomography (Wood, 1935). This chart, reproduced here as Figure 6, is recommended as a practical design aid.

It should be noted, by way of explanation of the chart, that the left-hand panel deals with sand-weight materials ($S_s = 2.65$). The internal pipe diameter appears on the left vertical axis, with V_{sm} on the central vertical axis. The particle diameter is plotted on a curve known, on the basis of its shape, as the "demi McDonald." This shape illustrates that for large particles, but not for small ones, the shear stress at the interface between the upper and lower layers increases with increasing particle size. Thus, for coarse-particle transport the velocity at the limit of deposition (i.e. the velocity beyond which no bed can remain stationary) will decrease with increasing particle size. This finding, which is amply supported by experimental evidence, shows how the fully-stratified mode of transport can display behavior quite different from that of the heterogeneous mode.

To demonstrate the particle size effect consider particles of $S_s = 2.65$ in a pipe 12 inches (0.30 m) in diameter. This diameter is located on the vertical scale on the left-hand side of the chart, and connected by straight-edge to any desired particle size on the curved scale. V_{sm} is then obtained by projected to the central vertical scale. For instance, a particle size of 0.025 in. (0.6 mm) gives V_{sm} of almost 13 ft/s (4 m/s), which is the largest value found for this pipe diameter and solids density. For a larger particle of, say 0.2 in. (5 mm), the deposition-limit velocity is diminished to about 9 ft/s (2.7 m/s).

When operating with centrifugal pumps it may be difficult to take advantage of the decrease of V_{sm} with increasing particle size. The question is one of obtaining a stable intercept of pump and pipeline characteristics, and will be discussed later in this section. For applications where control of particle size is limited, the conservative designer may wish simply to assume particles of "Murphian" size, i.e. those which give the largest value of V_{sm} for the pipe under consideration. In this case, it should be noted that the values of V_{sm} obtained from Figure 6 tend to be conservatively high, especially for large pipe diameters. Thus, these values can sometimes be used as operating velocities.

A particularly useful feature of nomographic presentation of results is that it gives an immediate indication of the sensitivity of the output to variations in the input. Thus on Figure 6 it is seen that the value of V_{sm} for sandweight solids in a 12 in. (0.30 m) pipe is

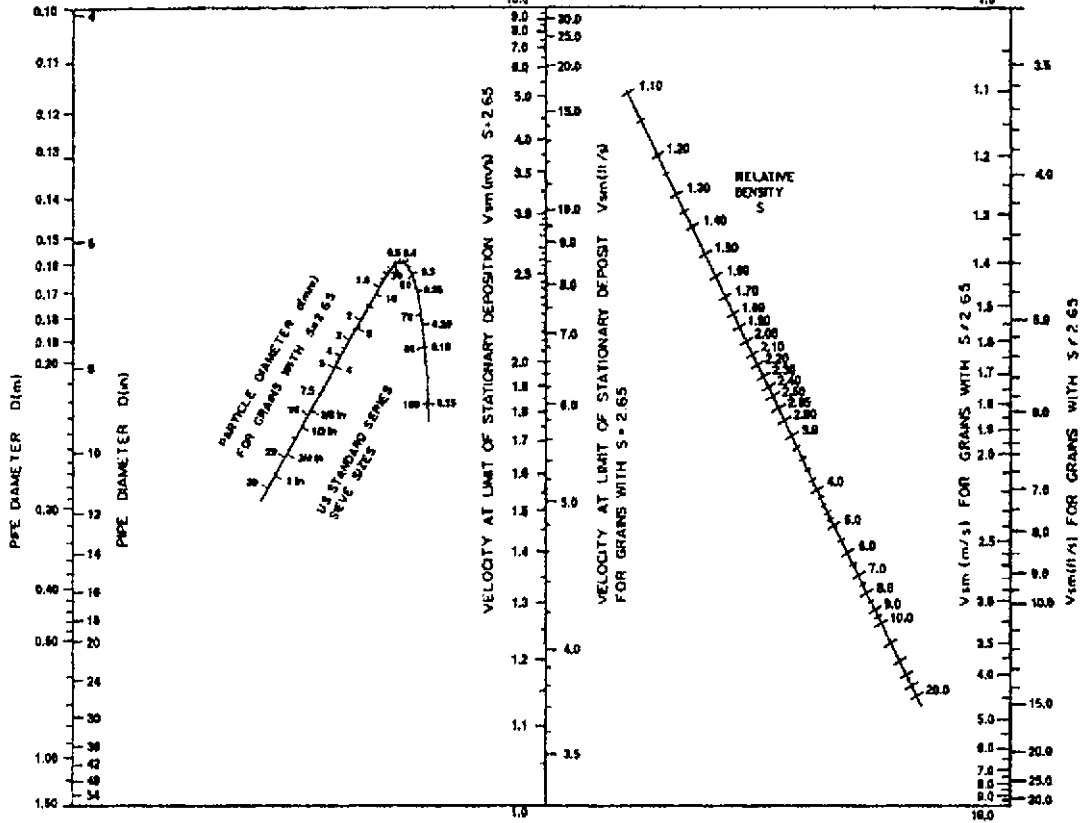

FIGURE 6 Nomographic chart for maximum velocity at limit of stationary deposition (from Wilson, 1979).

virtually unaffected by a variation of the particle diameter between 0.015 and 0.04 in. (0.4 and 1.0 mm). However, the right limb of the particle-diameter curve shows greatly increased sensitivity, so that a change in d from 0.006 to 0.008 in. (0.15 to 0.20 mm) alters V_{sm} by more than 25 percent.

It is found that a change of the relative density does not influence the form of the relation shown on Figure 6, but does require its "recalibration." This is accomplished graphically by using the inclined relative-density axis on the right-hand side of the figure. To illustrate the use of the right-hand panel of Figure 6, consider again the pipe 12 inches (0.30 m) in diameter, now carrying particles with a diameter of 0.004 in. (1.0 mm) and relative density 1.50. With 0.004 in. (1.0 mm) entered on the particle scale, a straight line joining it to the pipe diameter can be projected to the central axis of the figure, showing that V_{sm} is 11.5 ft/s (3.5 m/s) for the equivalent sand size. In order to correct this for the relative density of 1.50, the latter value is entered on the sloping axis on the right-hand side of the figure and joined by straight-edge to the point just found on the central axis (11.5 ft/s or 3.5 m/s). The projection of this line to the vertical axis on the right of the figure gives the adjusted value of the maximum deposition velocity, approximately 6 ft/s (1.9 m/s).

Particles that differ in density from sands may also have different values of other properties, including the solids fraction in the deposit and the mechanical friction coefficient between the particles and the pipe. The values of these quantities that were employed in the computer program, and hence are reflected in the nomographic chart, apply to sands but not necessarily to other materials. Therefore the values of V_{sm} determined from Figure 6 for materials other than sands must be treated as somewhat less accurate than values for sand. However, both the solids fraction in the bed and the particle-pipe mechanical friction coefficient occur in the computer program only as multiples of the submerged relative density of the particles, and it is found that any change in these quantities merely gives rise to a multiplicative factor which must be applied to the values of V_{sm} obtained from the figure. This permits calibration of the output of the nomographic chart from a few pilot-plant tests with the material of interest.

The particle diameter scale of Figure 6 has not been extended below 0.006 in. (0.15 mm) since smaller particles tend to be influenced by mechanisms not included in the mathematical model on which the nomogram is based. As shown by Thomas (1979) the viscous sublayer can have a significant effect, and all particles which are small enough to be completely embedded in this sublayer will behave in a fashion which is no longer dependent on particle diameter. In this limiting case certain simplifications can be made in the mathematical model. Thomas found that these lead to a simple expression for the shear velocity at the limit of stationary deposition, and on employing a power law approximation for the friction factor, he then obtained a corresponding expression for V_{sm}

$$V_{sm} = 9.0[g\nu(S_s - S_f)]^{0.37}(D/v)^{0.11} \tag{18}$$

Here ν represents the kinematic viscosity of the carrier fluid (i.e. μ/ρ), and the coefficient of 9.0 applies in any consistent system of units. This equation gives the minimum value of deposition velocity for small particles, assuming turbulent flow.

For cases where the interfacial friction sets up a sheared layer several grain diameters in thickness, a new analysis has been developed (Wilson, 1988; Wilson & Nnadi, 1990). For large pipes, and particles near the Murphian size, this new analysis shows that the particle size no longer influences V_{sm} directly. In such cases the value of V_{sm} is less than that predicted by Figure 6, a point which is in accord with experimental evidence. It is then necessary to obtain the value of V_{sm} from the new analysis of Interfacial friction, for comparison with the value from the nomographic chart.

When the parameters in the new analysis are given values typical for sands, it is found that the dimensionless maximum deposition velocity (i.e. the Durand deposition variable) depends only on the fluid friction factor for the portion of the pipe wall above the deposit. A power-law approximation gives an appropriate fit function for this effect, i.e.

$$\frac{(V_{sm})_{\max}}{\sqrt{2gD(S_s - S_f)}} = \left(\frac{0.018}{f_f}\right)^{0.13} \tag{19}$$

where f_f is the friction factor for fluid alone. If the value of V_{sm} found from the nomographic chart exceeds the value of $(V_{sm})_{max}$ from Eq. 19 the latter value should be used for V_{sm}.

Fully Stratified Coarse-Particle Transport Fully-stratified flow occurs where almost all of the particles travel as contact load (i.e. fluid suspension is ineffective). The ratio of particle diameter to pipe diameter is of major importance in determining the presence of this flow type, which does not normally occur for d/D ratios less than 0.015. Fully-stratified flow is less likely if the particles are broadly graded, especially if there is a significant homogeneous fraction (i.e. a significant fraction of particles smaller than 200 mesh/75 μm). Calculations made for narrow-graded slurries with water as a carrier fluid indicate fully-stratified behavior for values of d/D above 0.018.

Although the actual relationship of the detailed force-balance analysis cannot be expressed in closed form, simple approximating functions can be fitted to match the output of the detailed model. Wilson & Addie (1995) proposed the following expression for approximating fully-stratified flow:

$$\frac{i_m - i_w}{(S_m - 1)} = B'\left(\frac{V_m}{0.55V_{sm}}\right)^{-0.25} \tag{20}$$

The ratio on the left hand side of this equation is the same as that used by Newitt et al. (1955), and the right hand side shows the decrease of this ratio with increasing V_m/V_{sm}. The coefficient B' has a value of 1.0 for angular particles, and decreases with the degree of rounding. For typical cases the suggested default value is 0.75. As fully-stratified flow has higher energy consumption than other flow types, Eq. 20 can be thought of as representing the upper limit of excess pressure gradient (i.e. solids effect). Heterogeneous slurry flows, which are covered in the following section, will generally display smaller values of the solids effect.

Another type of stratified flow that may be encountered is flow above a stationary bed of solids. This type of operation is generally uneconomic, and thus is seldom a deliberate design choice, but it is sometimes found in existing pipelines. Flow over a stationary bed has been studied experimentally, and analyzed by a computer model (Nnadi & Wilson, 1992; Pugh, 1995). For most cases of this type of flow encountered in pipelines the following rough approximation to the computer output may be sufficient. It is based on particles near the "Murphian" size, which tend to be disproportionately represented in stationary deposits:

$$i_m = 0.32(S_s - 1)^{1.05}C_{vd}^{0.6}\left(\frac{V_m}{\sqrt{2gD}}\right)^{-0.1} \tag{21}$$

Pressure Gradients for Partially-Stratified Flow As mentioned previously, two methods of support are significant in partially-stratified flows: turbulent suspension and granular contact. For turbulent suspension the eddies can carry the particles with no significant additional energy consumption, but granular contacts set up Coulombic friction forces which must be overcome by an additional "solids effect" pressure gradient, represented by $(i_m - i_f)$ where i_f (or i_w) is the hydraulic gradient for fluid only. In many cases this solids effect varies with the submerged weight of solids, i.e. with $(S_s - S_f)C_v$ where S_f is the relative density of the fluid (1.0 for water) and C_v is the volumetric delivered concentration. The quantity $(S_s - S_f)C_v$ can also be expressed as $(S_m - S_f)$ where S_m is the relative density of the mixture. The relative solids effect, written $(i_m - i_f)/(S_m - S_f)$, can be obtained from pipe-loop testing. Typical results for partially-stratified flow are shown on Figure 7 for various concentrations of sand with d_{50} of 0.016 in. (0.42 mm). The relative solids effect drops with increasing mean velocity V_m, which in turn produces increased turbulent fluctuating velocities, implying that a larger fraction of particles will be suspended by turbulence. The straight fit line shown on the logarithmic coordinates of Figure 7 indicates that the relation can be approximated by a power law. (Other formulations have also been proposed, see for example Shook & Roco, 1992 and Gillies et al., 1991.)

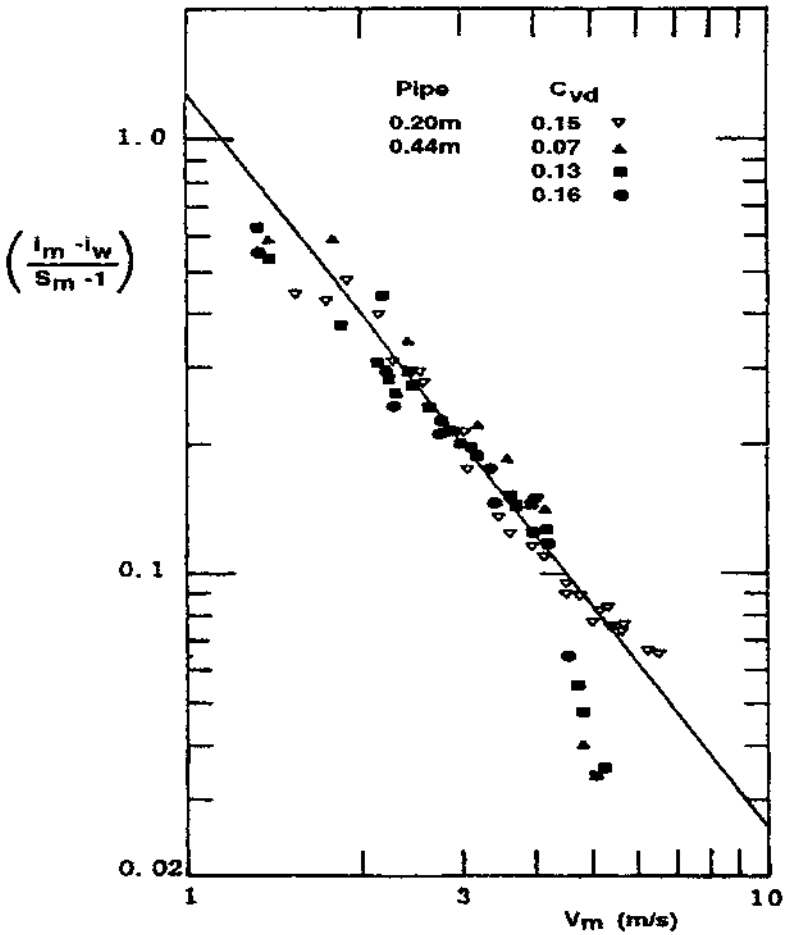

FIGURE 7 Behavior of masonry-sand slurry (d_{50} = 0.42 mm) in pipes of two sizes (after Clift et al., 1983). [m × 3.28 = ft; m/s × 3.28 = ft/s]

In addition to the slope parameter (denoted by M) a power law requires a central-value parameter, denoted here by V_{50}. Conceptually, this represents the value of V_m at which half the mass of solids is supported by granular contact and half by fluid suspension. From a practical standpoint it is necessary to match this point with a specific value of $(i_m - i_f)/(S_m - S_f)$. The mechanics of the situation were discussed by Wilson et al. (1997) who proposed a value of 0.22 and showed that this is suppoted by experimental data. The resulting equation is

$$\frac{(i_m - i_f)}{(S_m - S_f)} \cong 0.22\left(\frac{V_m}{V_{50}}\right)^{-M} \tag{22}$$

If test data are available, M and V_{50} can be obtained directly from the results. For example consider the data of Figure 7 in the 8 in. (0.20 m) pipe. In calculating the ratio $(i_m - i_w)/(S_m - 1)$, the clear water gradient i_w has been used to approximate i_f, and S_f is S_w,

i.e. 1.0. The value of i_w was calculated from the Darcy-Weisbach formula using the friction factor $f_f = 0.013$ measured previously for flows of water in this pipe. The plotted points fall on an essentially straight line on Figure 7. This behavior corresponds to Eq. 22. The slope of the line gives $M \approx 1.7$, which is typical for slurries with narrow particle grading. The point on the line where $(i_m - i_w)/(S_m - 1) = 0.22$ gives V_{50}, which is approximately 9 ft/s (2.8 m/s).

With V_{50} and M obtained for the 8 in. (0.20 m) pipe, scale-up to a larger pipe diameter can be carried out. The larger diameter of 18 in. (0.44 mm) has been selected because data are available with the same sand in this larger pipe (Clift et al., 1982) and thus the scaled-up results can be verified directly. In fact, as seen on Figure 7, the fit line for the larger pipe coincides with that for the smaller pipe in this instance. In this case the clear-water friction factor f_w was found to be the same for both pipes and in both pipes the particle size d was a small fraction of the pipe diameter. It has been found that V_{50} should vary with $(8/f_w)^{1/2}$; it should also depend on the diameter ratio d/D (Wilson & Watt, 1974; Wilson et al., 1997).

These factors can be incorporated in the scale-up procedure, which involves preparing curves of i_m versus V_m for various values of C_{vd} in the larger pipe, the relation for each line of constant C_{vd} being expressed as

$$i_m = \frac{f_w}{2gD} V_m^2 + 0.22(S_s - 1)V_{50}^M C_{vd} V_m^{-M} \tag{23}$$

It is typical to find a moderate decrease in f_w with increasing pipe size, which produces a small increase in V_{50}. Increases in D have the opposite effect, but for small ratios of d/D, as is the case for the data of Figure 7, this effect is not significant.

Other problems arise when pipeline experiments have not been carried out with the particular slurry of interest. In many cases of practical importance, information on the size and grading of the material to be pumped is limited, but estimates of the solids effect must be made. For example, consider the case of an ore that is to be crushed and then transported by pipeline. At the initial stage of the design there may be no adequate sample of the crushed ore, but estimates of the effect of the solids on the head loss must be made for feasibility studies, preliminary designs and cost estimates, and even for justifying the expenses of laboratory or pilot-plant testing.

To estimate the solids effect, two parameters are required: the power M and the velocity V_{50}. The value of M has a lower limit of 0.25 (for fully-stratified flow) and approaches 1.7 for slurries with narrow particle grading. If only a rough idea of the grading is available, it may be adequate to use the following approximation, which requires only an estimate of the particle diameter ratio d_{85}/d_{50} (d_{50} is the mass-median particle diameter and d_{85} is the diameter for which 85% by mass of the particles are smaller). Using this evaluation, the approximation for M is written

$$M \approx [\ell n(d_{85}/d_{50})]^{-1} \tag{24}$$

Here ℓn is the natural logarithm. Also, M should not be allowed to exceed 1.7 or fall below 0.25.

The next step is to obtain a commensurate approximation for V_{50} (Wilson et al., 1997). This formula reads

$$V_{50} \approx 3.93 d_{50}^{0.35}[(S_s - 1)/1.65]^{0.45} \tag{25}$$

Here d_{50} is in mm. The coefficient 3.93 applies for velocities in m/s; for velocities in ft/s this coefficient becomes 12.9. With sand-weight solids $(S_s - 1)$ equals 1.65 and the bracketed portion of Eq. 25 equals 1.00. The value of V_{50} obtained from Eq. 25 is substituted into Eq. 22 to obtain the solids effect $(i_m - i_f)$, where i_f is the gradient for an equal flow of water. Note, Eq. 25 is only applicable for 0.006 in $< d_{50} <$ 0.055 in (0.15 mm $< d_{50} <$ 1.4 mm). For larger particles the value of V_{50} given by Eq. 25 should be multiplied by $\cosh(60 d_{50}/D)$.

Remarks on Complex Slurry Flows In the introduction to this section, it was mentioned that slurry flows can be divided into three types on the basis of mechanisms of particle support. These types are homogeneous, partially-stratified and fully stratified, and

the applicable methods of analysis for these flows have been outlined in the appropriate preceding sections. Quite often, the particle grading curve is sufficiently broad to span two of the flow types, or even all three. This gives rise to complex slurry flows. The larger particles, which would settle readily in water, often receive considerable support from the smaller particles and the carrier fluid, promoting efficient transport. A complete analysis of such flows is not yet available, but it is hoped that the following remarks will aid the design engineer.

Whenever some coarse particles settle, they form contact load. As shown in earlier sections of this chapter, this has an effect on pressure drop which is quite different from that of particles suspended by the fluid. The contact-load effect, analyzed previously for the case of a Newtonian carrier fluid, must eventually be combined with the scaling laws for non-Newtonian fluids presented in an earlier part of this chapter. As laminar flows which have significant particle settling are usually avoided in design, only turbulent flows will be considered here.

Maciejewski et al. (1993) compared large-diameter transportation of coarse particles of about 4 in. (100 mm) in clay suspensions and in oil-sand tailings slurries (particle size below 0.03 in./0.8 mm). They found that the sand slurry was more effective as a transport medium than a viscous, homogeneous clay slurry. The important role of particles with sizes of 0.004 to 0.020 in. (0.1 to 0.5 mm) in reducing friction was further shown in studies by Sundqvist et al. (1996a, 1996b) for products with d_{50} of 0.024 to 0.027 in. (0.6 to 0.7 mm) and various size distributions, with maximum sizes of up to 6 in. (150 mm).

In studying the behavior of complex slurries like these, it is logical to begin by dividing the total concentration of solids C_v into three components, each associated with a support mechanism. Thus C_h stands for homogeneous, C_{mi} for partly stratified (the "middlings") and C_{cl} for the coarse fully stratified particles (the "clunkers"). On the basis outlined previously the particle size of 200 mesh (75 μm) separates C_h and C_{mi} and the size $0.018D$ separates C_{mi} and C_{cl}. This point is best illustrated by an example. Take $S_s = 2.65$; and a concentration of 30% by volume ($C_v = 0.30$). From the solids grading curve, suppose that 20% of the total is slimes, 50% middlings and 30% clunkers. Thus, the concentration of slimes in the slurry is $(0.30)(0.20) = 0.06$, and similarly 0.15 and 0.09 for middlings and clunkers, respectively. The equivalent fluid based on the slimes has specific gravity $S_h = 1 + (S_s - 1)C_h = 1 + (1.65)(0.06) = 1.099$ and that for the combined slimes and middlings is $S_{hmi} = 1 + (1.65)(.21) = 1.347$. Thus, for the middlings the specific gravity difference between solids and carrier fluid is $(2.650 - 1.099) = 1.551$ (rather than 1.650). For the clunkers, the equivalent difference is $(2.650 - 1.347) = 1.303$.

The homogeneous fraction now forms the carrier fluid for the rest of the slurry, and its hydraulic gradient i_h replaces i_w in equations like Eq. 20 and Eq. 22. These are used to determine the solids effect for middlings and clunkers, which may be written Δi_{mi} and Δi_{cl}. The gradient for the mixture i_m represents the sum of i_h and the solids effects for the middlings and the clunkers, i.e.

$$i_m = i_h + \Delta i_{mi} + \Delta i_{cl} \tag{26}$$

The homogeneous gradient i_h is based on appropriate equivalent-fluid or non-Newtonian calculations, as given previously. For the middlings, Δi_{mi} is effectively equivalent to $(i_m - i_f)$ in Eq. 22, when applied to the middlings only, giving

$$\Delta i_{mi} = C_{mi}(S_s - S_h)0.22\left(\frac{V_m}{V_{50}}\right)^{-M} \tag{27}$$

Here, S_h is the relative density of the homogeneous "carrier fluid" component (1.099 for the example just introduced). The evaluation of M and V_{50} will be mentioned in the following text.

For the clunkers, Δi_{cl} is based on Eq. 20, except that the carrier fluid for the clunkers now includes both the homogeneous portion and the middlings, with a relative density written S_{hmi} (1.347 for the example). The carrier fluid will also have an effect on the coefficient which will now be written B'' instead of B' (the evaluation of B'' will be mentioned next). The relation for Δi_{cl} is

$$\Delta i_{cl} = C_{cl}(S_s - S_{hmi})B''\left(\frac{V_m}{0.55V_{sm}}\right)^{-0.25} \tag{28}$$

For coarse solids only, it was suggested above that the parameter B' in Eq. 20 should have a default value of 0.75. When considerable fractions of middlings are found, B' must be reduced to give B''. As it is expected that the reduction is associated with density differences, the appropriate variable would appear to be the weight concentration, C_w, of fines plus middlings, i.e. C_{whmi} (for the example $C_{whmi} = 0.372$). Thus

$$B'' = B'(1 - \xi C_{whmi}) \tag{29}$$

where ξ is a coefficient with a proposed default value of unity.

Another point concerns the evaluation of V_{50} and M for the middlings. The methods of Eqs. 24 and 25 are basically applicable but d_{50} and d_{85} must now refer to the middlings fraction only, rather than the whole grading curve. For very broad well-distributed gradings the middlings will simply be a slice between 0.003 in. (0.075 mm) and $0.018D$. Here it may be possible to assume that d_{50} is the geometric mean of the two diameter limits (e.g. 0.025 in. for $D = 1$ ft or 0.64 mm for $D = 0.305$ m). For this case a default value of about 1.0 might be appropriate for M. V_{50} will be influenced by the rheological properties of the homogeneous fraction, which will influence the fall velocity of the middling particles, thus enhancing suspension. An initial approach is to consider the homogeneous part of the slurry to act as a Newtonian fluid with effective viscosity significantly higher than that of water. The effect of enhanced viscosity on V_{50} is of the form shown on Figure 8. On this figure the value of V_{50} based on water viscosity is entered on the abscissa (corrected for relative density of solids if different from 2.65). The various curves are for different μ_r, the ratio of viscosity to that of water at 70°F (20°C). The multiplier read from the ordinate can be applied to the V_{50} value for water to estimate V_{50} in the higher-viscosity carrier fluid.

EXAMPLE 2 This example pertains to fully-stratified flow of coarse magnetite particles ($d = 1$ in. or 25 mm). Because of their high relative density ($S_s = 4.4$) these particles are to be used as ballast for an offshore drilling rig. The magnetite will be transferred from ore carriers to the rig by a dredge pipeline with internal diameter 19.7 in. (0.500 m).

a. Find the deposition limit in this line, V_{sm}. Figure 6 is entered with the pipe diameter (on the left axis) and the particle diameter (on the demi McDonald).

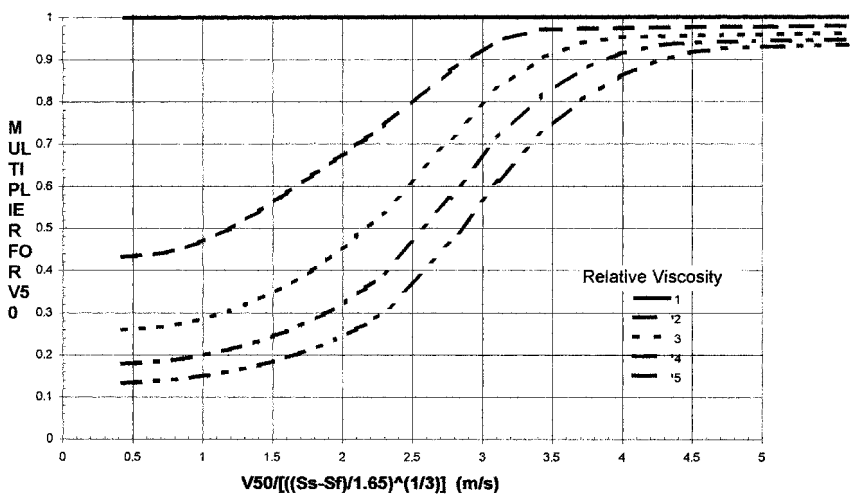

FIGURE 8 Variation of V_{50} with viscosity

Projection to the central axis gives V_{sm} = 8.7 ft/s (2.65 m/s) for sand-weight material. This number is joined to the relative density S (i.e. S_s) of 4.4 on the sloping axis and projected to the right-hand axis to give V_{sm} = 13 ft/s (4.0 m/s) for the magnetite.

b. Find the hydraulic gradient i_m for a volumetric solids concentration of 0.10 and a throughput velocity V_m = 16.4 ft/s (5.0 m/s). Assume rather angular material with B' = 0.9. The first step is to calculate the clear-water friction gradient of i_w. Using $f_w = 0.013$, i_w is given by $0.013V_m^2/2gD$ or 0.033 (height of water per length of pipe). To this must be added $(i_m - i_w)$, which Eq. 20 gives as $(S_m - 1)B'(V_m/0.55V_{sm})^{-0.25}$. The quantity $(S_m - 1)$ equals $C_v(S_s - 1)$ i.e. (0.10)(3.4) = 0.34. B' has been taken as 0.9 and the ratio $(V_m/0.55V_{sm})$ equals 2.27, giving $(i_m - i_w)$ = 0.250 and i_m = 0.28, i.e. 28 ft of water per 100 ft of line or 0.28 m of water per m of line. Very large gradients like this, which have been verified in prototype-scale testing, show why fully-stratified flow is only of interest for short-haul applications.

EXAMPLE 3

a. Suppose that the magnetite of the previous example has been ground to give d_{50} = 0.008 in. (0.20 mm) and d_{85} = 0.012 in. (0.30 mm). As in the previous example, D = 1.64 ft (0.50 m) and V_m = 16.4 ft/s (5.0 m/s). In this case the volumetric concentration C_v = 0.20. Find the V_{sm} and the hydraulic gradient i_m.

V_{sm} is found as in the previous example. The pipe size is joined to the particle size of 0.008 in. (0.20 mm) and projected to the central axis to give the deposition velocity for sand-weight solids. Solids specific gravity is entered on the sloping line, and projected to the right-hand axis to give V_{sm} = 14.4 ft/s (4.4 m/s). As in the previous example this is less than the proposed operating velocity, which is satisfactory.

The flow of this slurry will be partially stratified, and from Eq. 24, $M = [\ell n(0.30/0.20)]^{-1} = 2.5$. However, the maximum limit of M is 1.70, which will be used here. From Eq. 25,

$$V_{50} = 3.93(0.20)^{0.35}\left(\frac{3.40}{1.65}\right)^{0.45} = 3.1 \text{ m/s } (10 \text{ ft/s})$$

For this value of V_{50}, with M = 1.7 and V_m = 16.4 ft/s (5.0 m/s), the right hand side of Eq. 22 becomes 0.098. $(S_m - 1)$ equals $(S_s - 1)(C_v)$ = (3.40)(0.2) = 0.68. Hence
$i_m = i_w + (0.68)(0.098)$, and with i_w of 0.033 (found in Example 2) i_m is found to be 0.100 (ft water per ft or m water/m). Note that this gradient is only about one-third that for the coarse particles of the previous example, despite the fact that the solids concentration (and the tonnage transported) is twice as much.

b. As in part (a) but with d_{85} = 0.016 in. (0.40 mm). The power M is re-evaluated as $M = [\ell n(0.40/0.20)]^{-1} = 1.44$. For the unchanged values of V_{50} and V_m, the right-hand side of Eq. 22 becomes 0.110 and i_m equals 0.033 + 0.68 (.110) or 0.108 (ft water/ft or m water/m).

c. As in part (a) but assume that there is a fine-particle fraction that increases the viscosity of the homogeneous component to 4 times that of water. From part (a), M = 1.70 and V_{50} = 10 ft/s (3.1 m/s) in water. Adjusting for the density difference from the sand-water case gives the abscissa of Figure 8 as $3.1/(3.40/1.65)^{0.33}$ i.e. 7.88 ft/s (2.4 m/s). With this abscissa and a relative viscosity of 4, Figure 8 gives a multiple of 0.42, for a revised estimate of V_{50} as (0.42)(3.1) = 4.3 ft/s (1.3 m/s). Thus the right/hand side of Eq. 22 beocmes 0.022, and i_m = .033 + 0.015 or 0.048 (ft water/ft or m water/m). This revised estimate is only about one-half the value of 0.100 obtained in part (a) for pure water as the carrier fluid.

OTHER FACTORS

Vertical Flows For industrial application of vertical transportation of a solid-liquid mixture in a pipe, the operating velocity must be sufficient to maintain a continuous flow of solids at the discharge end. However, unnecessarily high velocity causes excessive pipe wear and energy losses. The appropriate operating velocity depends on the settling conditions of the solids, indicating that size, density, and concentration of particles are key parameters in the hydraulic design of a vertical particle-fluid transportation system.

Many experimental studies have been made of vertical slurry transport. For example, Sellgren (1979) used a pilot-scale facility with a centrifugal pump to investigate important design parameters for ores and industrial minerals taken from in-plant crushing and milling. The results of these experiments are summarized in the following paragraphs.

It is suggested that the allowable minimum mixture velocity be based on the settling velocity of the largest particles in still water multiplied by a factor of 4 or 5. Provided the velocity exceeds this value, then in most industrial applications, with volumetric concentrations of 15–30%, the corresponding pressure requirement in the vertical system can be determined by the equivalent-fluid model. As noted in connecetion with Eq. 5, this model is based on the density of the slurry and the friction factor for water. Applied to vertical flow, it gives

$$p = \rho_w g S_m z \left(1 + \frac{f_w V_m^2}{2gD} \right) \qquad (\text{for } V_m > V_{\text{all}}) \tag{30}$$

Here p is the pressure required, S_m is the relative density of the slurry, z is the length of vertical pipe, and V_{all} is the allowable minimum mixture velocity, approximately four times the settling velocity of the largest particle.

The settling velocity in still water of industrially-crushed mineral particles is normally reduced significantly compared to smooth spheres of corresponding size. Tests have shown that, on average the settling velocity for particles in the range of 0.04 in. to 1.2 in. (1 mm to 30 mm) is reduced approximately 50%. Therefore, the criterion previously given for the minimum allowable velocity could alternatively be formulated as: V_{all} is twice the settling velocity of a smooth sphere of the same size as the largest particles.

Within the constraints previously discussed, systems operate under conditions where the effect of relative velocity between the components appears to be negligible. The maximum particle sizes considered are in the range of 0.04 in. to 1.2 in. (1 mm to 30 mm) in pipe diameters of 4 to 12 in. (0.1 m to 0.3 m). With larger particle sizes (up to 4 to 6 in./100 to 150 mm) and low concentrations, the relative velocity between the components becomes significant. Boundary-layer transitional effects may also introduce certain instabilities that must be carefully evaluated in long vertical risers. Particles larger than one-fifth the pipe diameter can promote slugging instability in vertical hoisting, and particles larger than one-third the pipe diameter may jam the pipe and should be avoided.

EXAMPLE 4 Centrifual slurry pumps are used to pump a sand slurry (d_{50} = 0.06 in./1.5 mm) out of a quarry. The pipe is vertical with a length of 328 ft. (100 m) and a diameter of 4 in. (0.10 m). Tests have shown that the settling velocity of the largest particles is approximately 1.5 ft/s (0.45 m/s). Select the operating velocity and calculate the head requirement in meters of slurry.

Solution Following the guidelines previously given, the velocity V_{all} is four times 0.45, i.e. 6 ft/s (1.8 m/s). At this velocity, $V_m^2/2g$ is 0.54 ft (0.165 m). With the friction factor f_w taken as 0.016 for smooth-pipe conditions (see Figure 2), the head is obtained from Eq. 30 as

$$328 \left[1 + \frac{0.016(0.541)}{3.94/12} \right] = 336.5 \text{ ft of slurry}$$

in USCS units or 336.5 S_m in ft of water.

In SI units the calculation becomes

$$100\left[1 + \frac{0.016(0.165)}{0.1}\right] = 102.6 \text{ m of slurry}$$

or 102.6 S_m in meters of water.

Inclined Flows Lengths of pipe with an adverse slope often form part of pipelines transporting solids. Compared to the horizontal case, flow up an incline tends to require higher throughput velocities in order to avoid deposition. This is of greatest significance for coarse-particle flow.

In an experimental investigation carried out by Wilson & Tse (1984), four particle sizes between 0.04 and 0.24 in. (1 and 6 mm) were tested in a pipe at angles of inclination up to 40 degrees from the horizontal. It was found that the velocity at the limit of deposition initially increases with the angle of upward inclination, θ, reaching a maximum when this angle is about 30 degrees. For the materials tested this maximum velocity was approximately 50 percent larger than that required to move a deposit in a horizontal pipe. This large difference is clearly a matter of importance for both design and operation of pipelines with inclined sections.

As indicated schematically on Figure 1, V_{sm} marks the lower end of the range of desirable operating velocities for a pipeline. For purposes of comparison, it is appropriate to represent the deposition limit for inclined flow in terms of the dimensionless velocity, or Durand number, $V_{sm}/[2g(S_s - 1)D]^{1/2}$. The difference between the Durand number for inclined flow and that for horizontal flow, ΔD, is plotted against θ on Figure 9.

For the effect of pipe inclination on friction loss, the following widely-used formula by Worster & Denny (1955) may be employed for heterogeneous flows and homogeneous flows in which the hold-up effects are small. Their approach, based on water as the carrier fluid, deals with the extra pressure gradient ($\Delta i(\theta)$, expressed in height of water per length of pipe) beyond that for pumping water alone. For horizontal flow, this extra gradient is simply the solids effect ($i_m - i_w$), which may be written $\Delta i(0)$. Worster and Denny's formula states that

$$\Delta i(\theta) = \Delta i(0) cos\ \theta + (S_s - 1)C_{vd} \sin \theta \tag{31}$$

For highly stratified flows, Eq. 31 underestimates the losses. For further information see, for example, Wilson et al. (1997).

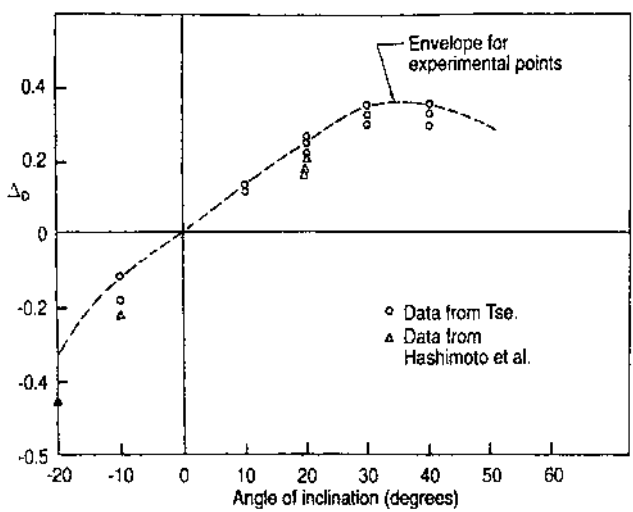

FIGURE 9 Effect of angle of inclination on Durand deposition parameter (after Wilson and Tse, 1984)

EXAMPLE 5 Consider an inclined suction pipe located on a dredge ladder. Pipe length = 59 ft (18 m), D = 25.6 in. (0.65 m), angle to the horizontal = 30°. Determine the deposition velocity and the head losses at the proposed operating velocity of 21.3 ft/s (6.5 m/s). Assume S_s = 2.65 and C_v = 0.20. For a horizontal pipe, it is calculated that V_{sm} = 15.7 ft/s (4.8 m/s) and at the proposed operating velocity i_w = 0.0373, $(i_m - i_w)$ = 0.0239.

Solution From Figure 9, at 30°, ΔD = 0.33, equivalent to an increase in V_{sm} of

$$0.33[(64.4) \cdot 1.65(25.6/12)]^{1/2} = 5.0 \text{ ft/s}$$

in USCS units, or

$$0.33[(19.62)(1.65)(0.65)]^{1/2} = 1.5 \text{ m/s}$$

in SI units.

The resulting limit velocity in the inclined pipe is 15.7 + 5.0 = 20.7 ft/s, 4.8 + 1.5 = 6.3 m/s, which is slightly less than the proposed operating velocity. At the operating velocity Eq. 31 gives the excess gradient, $\Delta i(30°)$, as

$$\Delta i(30°) = 0.0239 \cos 30° + (1.65(0.20) \sin 30°$$

where 0.0239 represents the solids effect in the horizontal pipe. Thus $\Delta i(30°)$ equals 0.0207 + 0.1650 or 0.1857. The clear water gradient i_w was 0.0373, giving a total value of 0.223, and on multiplying this by the suction-pipe length of 59 ft (18 m), the drop is found to be 13.2 ft (4.0 m) of water.

SYSTEM DESIGN AND ANALYSIS

Operating and Economic Considerations In order to compare the merits of different transport systems, it is necessary to have a measure of the energy required to move a given quantity of product over a given distance. In slurry transport, the solids are normally the "payload" while the conveying liquid is merely the "vehicle." The specific energy consumption is therefore to be related to the solids transported rather than to the mixture. However, the power which the pump must supply is used to drive the slurry as a whole, and is given by $\rho_w g Q_m H$ where H is the head in height of water and Q_m is the volumetric flow rate of the mixture. The payload of solids is delivered over the line length, L, at a volumetric rate that is the product of the delivered solids concentration C_{vd} and the mixture flow rate. If the application is a hoisting system, with the line directed vertically upwards, the rate at which energy is being added to the solids is $\rho_s g C_{vd} Q_m L$ or $\rho_w g S_s C_{vd} Q_m L$, and the efficiency of the system can be obtained by dividing the power input, giving $S_s C_{vd} L/H$. In this case the specific energy consumption is the inverse of the efficiency i.e.

$$\text{SEC} = \frac{H}{S_s C_{vd} L} \tag{33}$$

where, as before, H is the head supplied by the pump in height of water.

In the more usual case of an essentially horizontal pipeline, potential energy will not be added to the solids, and thus from the physicist's viewpoint no work will be done. However, in industrial practice transporting solids along the line represents useful work in the economic sense. We can no longer speak of efficiency in the physicist's terminology, but the appropriate economic measure of specific energy consumption is still given by Eq. 33. With H/L now equal to the friction gradient, i_m, the expression is written

$$\text{SEC} = \frac{i_m}{S_s C_{vd}} \tag{34}$$

To obtain a value in horsepower-hour/ton-mile, this ratio is multiplied by 5.33, and for kWh/tonne-km the factor is 2.73. If the power supplied to the pump is required, the expression must be divided by pump efficiency, and the efficiency of the drive train or motor can be taken into account in the same way.

The lower the SEC, the more energy-effective the pipeline is as a means of transport. Since S_s is fixed by the nature of the solids, the quotient i_m/C_{vd} is the basic variable to be considered.

Homogeneous Slurries Figure 10 is from Chapter 12 (written by Clift) of Wilson et al. (1997). The figure shows in simple generalized terms, the effect of changes in solids concentration on the resistance of a piping system to flow of a homogeneous, non-settling slurry. At velocities sufficiently high for the slurry to be in turbulent flow, the head lost in flowing through the system (measured as head of a fluid with the slurry density) can be estimated by treating the slurry as a fluid with an effectively constant friction factor, as shown in connection with Eq. 13. However, in laminar flow, to the left of the turbulent curve, the system head varies strongly with concentration, as shown schematically in Figure 10 where $C_1 < C_2 < C_3$. The transition between laminar and turbulent flow is indicated roughly by the intersection of the laminar system characteristic with the turbulent curve. Therefore, as illustrated, the transition velocity increases somewhat with solids concentration.

To examine the operability of such a system with centrifugal pumps, we now superimpose the pump head-discharge characteristic on to the system characteristic. For fine slurries the head delivered by the pump, evaluated in terms of the slurry density, is virtually unaffected by the solids. Therefore the characteristic of a fixed speed pump appears as a single curve in the coordinates of Figure 10, independent of slurry concentration.

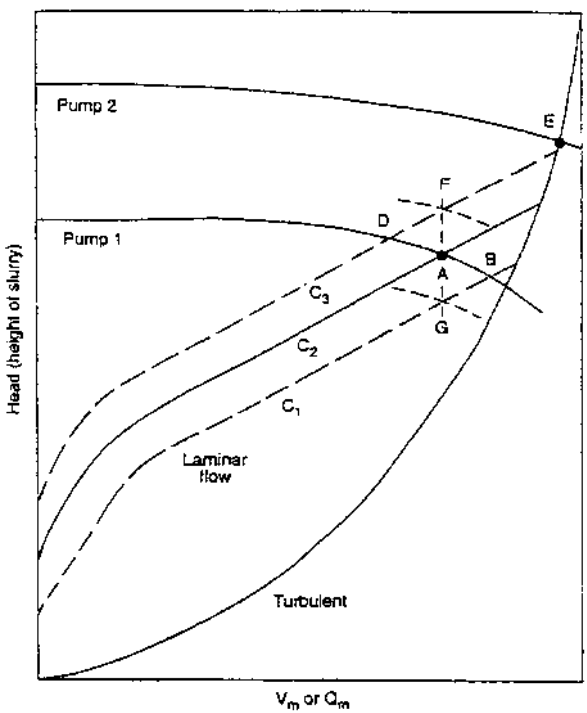

FIGURE 10 Schematic system and pump characteristics for flow of a homogeneous slurry at three concentrations (from Wilson *et al.*, 1997)

Consider first a system which has been designed to operate in the laminar range, corresponding to point A in Figure 10 with slurry concentration C_2. The curve labeled "Pump 1" represents the characteristic of a pump selected for this operating point.

Figure 10 shows the effect of varying solids concentrationl. If it decreases to C_1 then the system operating shifts to point B, the new intersection of the system and pump characteristics. Similarly, a concentration increase to C_2 shifts operation to point D. It was shown on Figure 3 that relatively small variations in concentration can have strong effects on the laminar flow curves. Thus the shifts from point A may result from quite small changes in slurry consistency. Nevertheless, as shown by Figure 10, the associated changes in mean velocity (and hence solids throughput) are amplified by the way the system and pump characteristics intersect. Thus steady operation in laminar flow with a fixed-speed centrifugal pump and with no flow control valve is possible only if the slurry consistency is tightly controlled.

For variable solids concentration, two alternatives are available. One is to operate in turbulent flow, at a point like E in Figure 10. "Pump 2" shows the head-discharge characteristics of a centrifugal pump selected for this duty. By operating on the turbulent system characteristic, variations in slurry consistency can be accommodated without significant changes in mixture velocity. This is probably the main reason why many designers prefer to use turbulent flow even for homogeneous slurries. The design point is then selected to be in the turbulent range for the highest solids concentration expected. However, it should be noted that this will not correspond to the lowest specific energy consumption. This is an example of the general point that design for variable operation is usually incompatible with design for minimum energy consumption.

The other option is to use a variable-speed pump. This is illustrated by points F and G in Figure 10. If the solids concentration increases from C_2 to C_3, then the pump speed is increased to keep a constant flow rate. The corresponding increase in pump speed raises the pump head-discharge characteristic to the broken curve shown passing through F. Similarly, if the concentration falls from C_2 to C_1, the pump is slowed down to give the characteristic passing through point G. Again, it must be noted that there is an economic penalty for designing for variable concentration, this time represented by the cost of the variable-speed drive and the energy losses in the drive train.

Settling Slurries We now turn to problems of system operability for settling slurries. (For a more detailed treatment see Wilson et al., 1997.) Figure 11 shows typical "system characteristics" for a settling slurry at three delivered concentrations, in terms of head of slurry, j_m. Only the frictional contribution for horizontal transport is considered here. The form of the system characteristics is typical of heterogeneous flow of a settling slurry. The three slurry characteristics are scaled for three notional delivered relative densities, i.e. three values of S_{md}. The slurry curves all show the minimia typical of a heterogeneous slurry flow. As is typical for heterogeneous slurries, the minimum friction gradient occurs at velocities above the deposition point and the position of the minimum moves to somewhat higher velocities as the solids concentration increases.

Figure 11 also shows the point where j_m equals i_w. At this crossing point (but not elsewhere) the heterogeneous slurry behaves like an "equivalent fluid," with a value of 1.0 for the coefficient A' in the homogeneous-flow equation (Eq. 5).

It is now appropriate to consider the behavior of this system with one or more variable-speed centrifugal pumps, with characteristics shown in Figure 11 as "Pump (water" and "Pump (mixture)." The latter decreases with increasing concentration, due to the effects of solids on pump performance discussed earlier in this section. Therefore, to maintain a constant head and flow rate at point A in Figure 11, the pump rotational speed must be adjusted for the actual solids concentration.

It sometimes happens in industrial practice that the pipeline characteristics for different concentrations cross over at a single point at the water curve and at a suitable operating velocity, as shown schematically in Figure 11. This behavior is expected for closely-graded materials with volumetric concentrations less than 20%, but may not apply for broad gradings or higher concentrations. The results with the broadly-graded sand in Table 3 show that j_m was approximately constant (equal to 0.055 over a concentration range 20% to 40%) for the selected velocity = 15 ft/s (4.5 m/s). However, the operating point

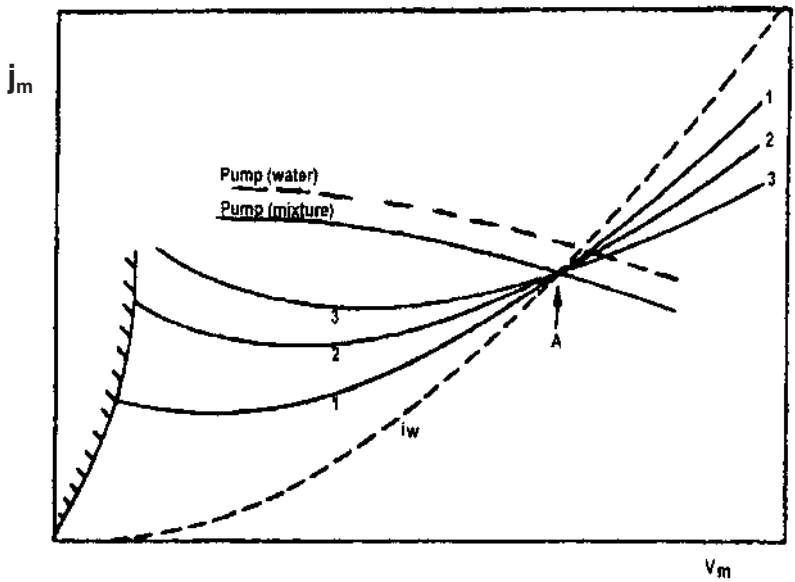

FIGURE 11 Schmematic system and pump characteristics for heterogeneous (settling) slurry flow at various delivered concentrations (after Wilson *et al.*, 1997)

TABLE 3 Comparison of slurry friction losses and water friction losses for a broadly graded sand with $d_{85}/d_{50} \approx 7.1$. Data from Sundqvist et al. (1996a)

Product	Sand		
Max. particle size, in. (mm)		0.4 (10)	
Average, d_{50}, in. (mm)		0.025 (0.65)	
Portion of fine particles, X_h%		0	
Pipeline—Diameter, in. (m)		12 (0.3)	
Velocity, ft/s (m/s)		15 (4.5)	
Water friction losses, i_w		0.041	
Conc. by volume, C_v	0.20	0.30	0.40
Slurry friction losses, j_m	0.055	0.055	0.055

was not located on the water curve ($i_w = 0.041$). It follows from Table 3 that the slurry friction losses, j_m, exceeded the corresponding water losses, i_w, by 35%.

The operating data for the sand in Table 3 are of great practical interest since they demonstrate the energy-efficiency of transporting this product at very high solids concentrations. Experiments by Sellgren & Addie (1993) with this sand indicated that the pump solids effect was not influenced greatly by increased solids concentrations. For the highest concentration studied here, the maximum values of R_H and R_η were estimated to be 13 and 15%, respectively. An example including pipeline friction and the effect of solids on the water efficiency of the pump is given in Table 4.

It follows that the energy required to overcome friction losses decreased from 0.039 to 0.024 HPh/ton (0.032 to 0.020 kWh/tonne) when C_{vd} was increased from 20 to 40%. The decrease corresponds to about 37%. The capacity of the pipeline is in this case doubled by the increase in concentration. Because the pump solids effect for this product and pump

TABLE 4 Data for the sand slurry of Table 3 in a 12 in. (0.3 m) diameter pipe using a 14 in. (0.35 m) by 12 in. (0.3 m) conventional heavy-duty pump with an impeller diameter of 36 in. (0.91 m). Pipeline length = 852 ft (260 m), flow rate = 5200 US gpm (328 l/s) and velocity = 15 ft/s (4.5 m/s). Volumetric concentrations 20, 30 and 40% (from Sellgren and Addie, 1996)

	Concentrations by volume (%)		
	20	30	40
Capacity, ton/h (tonne/h)	690 (627)	1035 (941)	1380 (1255)
Energy to overcome pipeline friction, HPh/ton (kWh/tonne)	0.039 (0.032)	0.029 (0.024)	0.024 (0.020)
Pump head reduction, R_H (%)	8	11	13
Required rotary speed (rpm)	333	338	342
Pump water efficiency (%)	79.5	79.4	79.3
Pump efficiency reduction, R_η (%)	6	11	15
Pump efficiency (%)	74.8	70.7	67.4
Total energy, HPh/ton (kWh/tonne)	0.052 (0.043)	0.041 (0.034)	0.037 (0.030)

remained fairly moderate also for the highest concentration, the total energy requirement per tonne decreased from 0.052 to 0.037 (0.043 to 0.030) with an increased C_{vd} value from 20 to 40%. The lowering then corresponds to about 30%.

The attrition of coarse and angular particles during circulation in a test-loop may have a strong influence on friction losses and pump performance. However, the results in Tables 3 and 4 with high solids concentrations and coarse particles embedded in a sand slurry are not expected to have been significantly influenced by circulation effects. In large-scale loop testing special loading and quick measurement procedures are now used to evaluate the interaction of particle attrition, pipeline friction and pump performance. In general, designing a system to transport a slurry combining broad grading and high concentration requires pilot plant testing using the same material that will be pumped in the prototype line.

The solids concentration used throughout this section (denoted C_v or C_{vd}) refers to delivered concentration, and this is incorporated in the design-oriented equations. Large particles tend to have a lower velocity than small ones, and thus a larger resident (*in situ*) concentration in the pipeline, and this feature should also be considered in designing once-through pipelines on the basis of recirculating test-loop data.

For long-distance freight pipelines it is worthwhile to devote considerable effort to preparing and controlling slurry properties. For such lines solids concentrations range from 0.25 (25%) for ores with S_s of, say, 5.0, to 0.40 (40%) for coal with S_s = 1.4. Velocities are usually maintained below 6.6 ft/s (2.0 m/s). For a typical 10 in. (0.25 m) pipe, annual throughput of solids range from about 2.8 M tons (2.8 M tonnes) for ore to 1.4 M tons (1.3 M tonnes) for coal. The corresponding specific energy consumption, including a total pump and drive-train efficiency of 75%, are respectively, 0.13 and 0.17 HPh/ton-mile (0.065 and 0.085 kWh/ton-km). For such cases the energy cost for pumping amounts to roughly half the annual operating cost. This cost is, say, 20% to 30% of the total annual cost, which is seen to be dominated by repayment of capital expenditure.

REFERENCES

Blatch, N. S. (1906). Discussion of "Works for the purification of the water supply of Washington D.C." (Hazen, A. and Hardy, E. D.) *Trans Amer. Soc. Civil Engrs.* Vol. 57, pp. 400–409.

Brown, N. & Heywood, N. (1992). *Slurry Handling Design of Solid-Liquid Systems.* Elsevier Science Publishers, United Kingdom.

Carstens, M. R. & Addie, G. R. (1981). A sand-water slurry experiment. *Jour. Hydr. Div.* ASCE, Vol. 107, No. HY4, pp. 501–507.

Clift, R. Wilson, K. C., Addie, G. R. and Carstens, M. R. (1982). A mechanisitically-based method for scaling pipeline tests for settling slurries.

Durand, R. (1951a). Transport hydraulique des matériaux solides en conduite, études expérimentales pour les cendres de la central Arrighi. *Houille Blanche,* Vol. 6, No. 3, pp. 384–393.

Durand, R. (1951b). Transport hydraulique des graviers et galets en conduite. *Houille Blanche,* Vol. 6, No. B, pp. 609–619.

Gillies, R. G., Shook, C. A. and Wilson, K. C. (1991). An improved two layer model for horizontal slurry pipeline flow. *Canad. J. Chem. Engng.,* **69,** 173–178.

Hedström, B. O. A. (1952). Flow of plastics materials in pipes. *Ind. and Eng. Chem.,* Vol. 44, No. 3, pp. 651–656.

Kostuik, S. P. (1966). Hydraulic hoisting and pilot-plant investigation of the pipeline transport of crushed magnetite. *The Canadian Mining and Metallurgical Bulletin,* January, 25–38.

Lumley, J. L. (1973). Drag reduction in turbulent flow by polymer additives, *J. Poly Sci., Macromol, Rev. 7,* A. Peterlin (Ed.), Interscience, New York, pp. 263–290 (1973).

Lumley, J. L. (1978). Two-phase flow and non-Newtonian flow. In *Turbulence,* P. Bradshaw (Ed.), Tiopics in Applied Physics, Vol. 12, Springer-Verlag, Berlin (1978), Chapter 7.

Maciejewski, W., Oxenford, J. and Shook, C. (1993). Transport of Coarse Rock with Sand and Clay Slurries, Hydrotransport, 12, Brügge, Belgium, pp. 705–724.

Mooney, M. (1931). Explicit formulas for slip and fluidity. *J. Rheol.* Vol. 2, p. 210 ff.

Newitt, D. M., Richardson, J. F., Abbot, M., & Turtle, R. B. (1955). Hydraulic conveying of solids in horizontal pipes. *Trans. Inst. of Chem. Engrs.,* Vol. 33, London, U.K.

Nnadi, F. N. & Wilson, K. C. (1992). Motion of contact load at high shear stress. *J. Hydr. Engrg.,* ASCE **118** (12), pp. 1670–1684.

Pugh, F. J. (1995). *Bed-load Velocity and Concentration Profiles in High Shear Stress Flows.* Ph.D. Thesis, Queen's University, Canada.

Rabinowitsch, B. (1929). Über die Viscosität von Solen. *Zeitschrift physik. Chem.,* **A 145,** p. 1 ff.

Sellgren, A. & Addie, G. (1996). Pump and pipleine solids effects of transporting sands with different size distributions and concentrations. *Proc. 13th Int. Conference on the Hydraulic Transport of Solids in Pipes,* Johannesburg, South Africa, pp. 227–236.

Sellgren, A. & Addie, G. (1998). Effective integrated mine waste handling with slurry pumping. *Proceedings Fifth International Conference on Tailings and Mine Waste.* January 26–28, Ft. Collins, USA, pp. 103–107.

Shook, C. A. and Roco, M. C. (1991). *Slurry Flow Principles and Practice.* Butterworth-Heinemann.

Sundqvist, A., Sellgren, A. and Addie, G. R. (1996a). Pipeline friction losses of coarse and slurries: comparison with a design model, in *Powder Technology,* **89,** pp. 9–18.

Sundqvist, A., Sellgren, A. and Addie, G. R. (1996b). Slurry pipeline friction losses for coarse and high-density industrial products, in *Powder Technology,* **89,** pp. 19–28.

Thomas, A. D. (1979). The role of laminar/turbulent transition in determining the critical deposit velocity and the operating pressure gradient for long distance slurry pipelines, *Proc. Hydrotransport 6,* BHRA Fluid Engineering, Cranfield, UK, pp. 13–26.

Thomas, D. G. (1963). Non-Newtonian suspensions. Part 1, physical properties and laminar transport characteristics. *Ind. and Eng. Chem.* Vol. 55, No. 11, pp. 18–29.

Thomas, A. D. & Wilson, K. C. (1987). New analysis of non-Newtonian turbulent flow—yield-power-law fluids. *Canad. J. Chem. Engrg.,* Vol. 65, pp. 335–338.

Wilson, K. C. (1979). Deposition-limit nomograms for particles of various densities in pipeline flow, *Proc. Hydrotransport 6,* BHRA Fluid Engineering, Cranfield, UK, pp. 1–12.

Wilson, K. C. (1986). Modelling the effects of non-Newtonian and time-dependent slurry behavior. *Proc. Hydrotransport 10,* BHRA Fluid Engineering, Cranfield, UK, pp. 283–289.

Wilson, K. C. (1988). Evaluation of interfacial friction for pipeline transport models. *Proc. Hydrotransport 11,* BHRA Fluid Engineering, Cranfield, UK, pp. 107–116.

Wilson, K. C. (1989). Two mechanisms for drag reduction. *Drag Reduction in Fluid Flows, Techniques for Friction Control,* Ed. H. R. J. Sellina nd R. T. Moses, pp. 1–8. Ellis Horwood Ltd., Chichester, UK.

Wilson, K. C. & Addie, G. R. (1995). Coarse-particle pipeline transport: effect of particle degradation on friction. *Proc. 8th International Freight Pipeline Society Symposium,* pp. 151–156.

Wilson, K. C., & Judge, D. G. (1978). Analytically-based nomographic charts for sand-water flow, *Proc. Hydrotransport 5,* Solids in Pipes, BHRA Fluid Engineering, Cranfield, UK, pp. A1-1–11.

Wilson, K. C., & Nnadi, F. N. (1990). Behavior of mobile beds at high shear stress. *Proc. 22nd Int'l Conference on Coastal Engineering,* Delft, Netherlands, Vol. 3, pp. 2536–2541.

Wilson, K. C., & Thomas, A. D. (1985). A new analysis of the turbulent flow of non-Newtonian fluids. *Canad. J. Chem. Engrg.,* Vol. 63, pp. 539–546.

Wilson, K. C., & Tse, J. K. P. (1984). Deposition limit for coarse-particle transport in inclined pipes. *Proc. Hydrotransport 9,* BHRA Fluid Engineering, Cranfield, UK, pp. 149–169.

Wilson, K. C. & Watt, W. E. (1974). Influence of particle diameter on the turbulent support of solids in pipeline flow. *Prod. Hydrotransport 3,* BHRA Fluid Engineering, Cranfield, UK, pp. E1-1–E1-13.

Wilson, K. C., Addie, G. R., Sellgren, A. and Clift, R. (1997). *Slurry Transport Using Centrifugal Pumps, 2nd Ed.* Blackie (Chapman & Hall).

Wood, F. M. (1935). Standard nomographic forms for equations in three variables, *Canadian Journal of Research,* Vol. 12.